SYNCHRONIZATION OF CHAOS AND THE TRANSITION TO WAVE TURBULENCE

R. L. VIANA and S. R. LOPES
Department of Physics, Federal University of Paraná,
81531-990 Curitiba, Paraná, Brazil

J. D. SZEZECH Jr. and I. L. CALDAS
Institute of Physics, University of São Paulo,
05315-970 São Paulo, São Paulo, Brazil

We investigated the transition to wave turbulence in a spatially extended three-wave interacting model, where a spatially homogeneous state undergoing chaotic dynamics undergoes spatial mode excitation. The transition to this weakly turbulent state can be regarded as the loss of synchronization of chaos of mode oscillators describing the spatial dynamics.

Keywords: Synchronization of chaos; wave turbulence; onset of turbulence.

1. Introduction

The onset of turbulence is one of the outstanding problems of theoretical physics [Landau & Lifshitz, 1987; Frisch, 1995]. A seminal contribution to this study was brought about by Ruelle and Takens, who described the onset of turbulence as a sequence of Hopf bifurcations yielding a chaotic attractor in the system phase space [Ruelle & Takens, 1971; Newhouse *et al.*, 1978]. In spite of the recent progress in turbulence theory, wave turbulence still presents a number of theoretical challenges, one of them being the onset of turbulence. Wave turbulence occurs in systems of nonlinear dispersive waves, where energy transfer occurs chiefly among resonant sets of waves [Zakharov *et al.*, 2004]. Wave turbulence is present in a plethora of physically relevant systems like capillary waves [Schröder *et al.*, 1996], magnetized plasmas [Musher *et al.*, 1995], superfluid helium [Kolmakov & Pokrowsky, 1995], nonlinear optics [Dyachenko *et al.*, 1992], acoustic waves [Zakharov & Sagdeev, 1970], astrophysics [Sridhar & Goldreich, 1994], among others.

In most applications of wave turbulence, the wave amplitudes are relatively weak, such that only quadratic nonlinearities need to be considered. Hence the dynamical features of more complicated models can be retained by simpler models, like the resonant three-wave interacting wave [Kaup *et al.*, 1979]. Such system occurs in fluid dynamics [Turner, 1996; Li, 2007], plasma physics [Chian *et al.*, 1994; Chian & Rizzato, 1994] and nonlinear optics [Rundquist *et al.*, 1998; Stegeman & Segev, 1999; Picozzi & Haeltermann, 2001]. The nonlinear three-wave model describes the exchange of energy among a high-frequency (parent) wave and its sideband (daughters) with quadratic interactions, as well as with a spatial diffusion term. The model yet contains an energy source term which can be phenomenologically introduced from a linear growth rate for the parent wave.

We identify the onset of wave turbulence as the excitation of spatial Fourier modes, in the presence of an underlying temporally chaotic dynamics. This approach can be pursued numerically by making a pseudo-spectral decomposition of the wave field. This procedure converts the nonlinear partial differential equation into a system of coupled nonlinear ordinary differential equations governing

the time evolution of the Fourier mode amplitudes. In the language of Fourier phase space, where the state variables are the Fourier mode amplitudes, we can assign the underlying chaotic dynamics to the existence of a strange attractor immersed in a low-dimensional subspace of the phase space, which we call a homogeneous manifold. The spatial modes correspond, in this description, to variables representing directions transversal to this homogeneous manifold. The excitation of spatial modes following the onset of wave turbulence is observed as relatively sharp spikes in the corresponding modes for the three waves. We have found that such intermittent spikes have a statistical distribution characteristic of the so-called on–off intermittency [Szezech Jr. *et al.*, 2007; Szezech Jr. *et al.*, 2009]. Because of the spikes observed just after the onset of turbulence, the latter can be called a bubbling transition.

In this paper, we aim to describe the onset of wave turbulence in the nonlinear three-wave interaction model by using the concept of synchronization. Synchronization of chaotic motion is an intensively studied subject, following the pioneer work of Fujisaka and Yamada [1983], Afraimovich *et al.* [1986] and Pecora and Carroll [1990]. In general terms, synchronization is a process of adjustment of rhythms of oscillators due to their interactions, which can occur even if their dynamics is chaotic [Pikovsky *et al.*, 2001]. Synchronization of chaos has been observed in both numerical and laboratory experiments. We are particularly interested in chaotic phase synchronization, for which we can define a geometrical phase to each oscillator, in such a way that, due to the interaction between the oscillators, their phases are equal, whereas their amplitudes may not remain correlated at all.

Before the transition to wave turbulence, the wave amplitudes (in the real space, rather than in the Fourier mode amplitude space) are spatially homogeneous. Since we have performed a pseudospectral Fourier expansion with a finite number of modes, we have the same number of discretized points in the real space. In the spatially homogeneous state, each spatial point can be regarded as a nonlinear oscillator. This behavior turns out to be similar to relaxation oscillations observed in self-sustained systems of the type described by the van der Pol equation. Due to the temporally chaotic dynamics which pumps the time evolution of spatial mode amplitudes, a spatially homogeneous state

can be regarded as a set of chaotic oscillators exhibiting phase synchronization. If the oscillators lose phase synchronization, there is spatial mode excitation and turbulent behavior sets in. Hence, it is possible to investigate the onset of bubbling by applying numerical diagnostics of chaotic phase synchronization.

The rest of this paper is organized as follows: Sec. 2 describes the spatially extended three-wave interacting model and the Fourier mode expansion we create in order to work with a set of ordinary differential equations governing the time evolution of the amplitudes. Section 3 is devoted to discussing the concept of chaotic phase synchronization and how it relates with the excitation of spatial modes, as well as the first positive Lyapunov exponents and their finite-time fluctuations. Our conclusions appear in the last section.

2. Spatially Extended Three-Wave Interacting Model

We will study a paradigmatic model of low-dimensional chaos, which consists of three dispersive monochromatic waves propagating along the x-direction, whose complex amplitudes are denoted A_α, $\alpha = 1, 2, 3$. These waves form a triplet, for their wave numbers and frequencies must satisfy resonance conditions

$$\mathbf{k}_3 = \mathbf{k}_1 + \mathbf{k}_2, \tag{1}$$

$$\Omega_{\mathbf{k}_3} = \Omega_{\mathbf{k}_1} - \Omega_{\mathbf{k}_2} - \delta, \tag{2}$$

where δ is a small frequency mismatch introduced because the frequencies obtained from the linear dispersion relations may not be matched even for perfectly matched wave vectors. This effect occurs quite often in laser–plasma interactions, where it can enhance the linear growth rate [Lopes & Rizzato, 1999]. For the same token, wave vector mismatches could also be taken into account, but since it is formally equivalent to frequency mismatch it suffices to analyze the latter.

Each wave has a constant group velocity $v_{g\alpha} = d\Omega_{\mathbf{k}_\alpha}/dk_\alpha$, given by its linear dispersion relation, and we shall assume in this paper that $v_{g2} > v_{g1} > v_{g3}$. This is consistent with a scenario where $A_1(x,t)$ stands for the parent wave amplitude, $A_2(x,t)$ and $A_3(x,t)$ being the corresponding quantities for the faster and slower daughter waves, respectively [Kaup *et al.*, 1979]. In the case of nonlinear wave

interactions in nonmagnetized plasmas, A_1 may stand, for example, for a transverse electromagnetic wave, A_2 an ion-acoustic wave, and A_3 is a Langmuir wave (anti-Stokes mode) [Chian *et al.*, 1994].

We also suppose that the nonlinearities present in the wave interactions are sufficiently weak, such that only quadratic terms in the wave amplitudes need to be considered. In this case, the three-wave system can be described by the following Hamiltonian density [Lopes & Rizzato, 1999]

$$\mathcal{H} = -A_1 A_2^* A_3^* + A_1^* A_2 A_3 + i\delta |A_3|^2$$
$$- \sum_{\alpha=1}^{3} v_{g\alpha} A_\alpha^* \frac{\partial A_\alpha}{\partial x}, \qquad (3)$$

such that the equations governing the spatiotemporal dynamics of the system are obtained from

$$\frac{\partial A_\alpha}{\partial t} = \frac{\delta H}{\delta A_\alpha^*}, \qquad (4)$$

$$\frac{\partial A_\alpha^*}{\partial t} = -\frac{\delta H}{\delta A_\alpha}, \qquad (5)$$

where $H = \int dx \mathcal{H}$ and the functional derivative is

$$\frac{\delta}{\delta A_\alpha} \equiv \frac{\partial}{\partial A_\alpha} - \frac{\partial}{\partial x} \frac{\partial}{\partial \left(\frac{\partial A_\alpha}{\partial x} \right)}. \qquad (6)$$

Since the Hamiltonian H does not depend explicitly on time, it is a conserved quantity. We can introduce phenomenologically wave growth and dissipation by adding growth and decay rates: the coefficients $\nu_1 > 0$ and $\nu_{2,3} < 0$ represent energy injection (through wave 1) and dissipation (through waves 2 and 3), respectively. This sign convention follows from a linear analysis in which the parent wave is supposed to grow exponentially with time, whereas the daughter waves are expected to decay exponentially in each cycle. Diffusion is also introduced by a Laplacian term in the parent wave, which provides a cutoff in the linear wave growth, being essential to nonlinear saturation

With such modifications, the equations governing the dynamics of the resonant three-wave interaction are [Kaup *et al.*, 1979; Chow *et al.*, 1992]

$$\frac{\partial A_1}{\partial t} + v_{g1} \frac{\partial A_1}{\partial x} = A_2 A_3 + \nu_1 A_1 + D \frac{\partial^2 A_1}{\partial x^2}, \quad (7)$$

$$\frac{\partial A_2}{\partial t} + v_{g2} \frac{\partial A_2}{\partial x} = -A_1 A_3^* + \nu_2 A_2, \qquad (8)$$

$$\frac{\partial A_3}{\partial t} + v_{g3} \frac{\partial A_3}{\partial x} = i\delta A_3 - A_1 A_2^* + \nu_3 A_3, \qquad (9)$$

where D is a diffusion coefficient.

We perform a Fourier decomposition in the wave amplitudes by using a one-dimensional box of length L with periodic boundary conditions and retaining N modes.

$$A_\alpha(x,t) = \sum_{n=-(N/2)+1}^{N/2} |a_{\alpha,n}(t)|$$
$$\times \exp\{i[\kappa_{\alpha,n} x + \phi_{\alpha,n}(t)]\}, \quad (\alpha = 1, 2, 3), \qquad (10)$$

where $a_{\alpha,n}(t)$ is the time-dependent Fourier coefficient corresponding to the mode number

$$\kappa_{\alpha,n} = \frac{2\pi n}{L}. \qquad (11)$$

The time evolution of these Fourier mode amplitudes are governed by a truncated system of $3N$ coupled ordinary differential equations

$$\dot{a}_{1_n}(t) = (\nu_1 - iv_{g1}k_n - Dk_n{}^2)a_{1_n} + \mathcal{F}[A_2 A_3], \qquad (12)$$

$$\dot{a}_{2_n}(t) = (\nu_2 - iv_{g2})a_{2_n} - \mathcal{F}[A_1 A_3^*], \qquad (13)$$

$$\dot{a}_{3_n}(t) = (\nu_3 - iv_{g3}k_n + i\delta_3)a_{3_n} - \mathcal{F}[A_1 A_2^*], \qquad (14)$$

where the symbol $\mathcal{F}$ denotes the discrete Fourier transform (actually computed from the FFT algorithm). This is so because the product of wave amplitudes is computed faster in the real space (even taking into account two calls to FFT routine) than in Fourier space (where it would need a time-consuming convolution integral). The parent wave has a positive linear growth rate and pumps energy to the daughter waves. We kept the group velocities, frequency mismatch, and diffusion coefficient at fixed values: $v_{g1} = 0.0$, $v_{g2} = 1.0$, $v_{g3} = -1.0$, $\delta = 0.1$, and $D = 1.0$, respectively, corresponding to the so-called solitonic regime [Kaup *et al.*, 1979]. The growth rate will be fixed as $\nu_1 = 0.1$, and the decay rate $\nu_2 = \nu_3$ are negative, the tunable parameter being used.

The box length was chosen such that $L = 2\pi / \kappa_{1,1} = 2\pi/0.89$. The initial conditions were chosen

R. L. Viana et al.

as $F_{1,0}(0) = 0.500 + i0.000$, and $F_{2,\pm1}(0) = 0.001 + i0.001$, where

$$F_{\alpha,n}(t) = a_{\alpha,n}(t)e^{i\phi_{\alpha,n}(t)}, \qquad (15)$$

all the other modes being set to zero.

3. Synchronization of Oscillators and the Excitation of Spatial Modes

The system (12)–(14) was numerically integrated using routines from the LSODE package [Hindmarch, 1983], yielding a set of $3N$ complex mode amplitudes $a_{\alpha,n}(t)$ in Fourier space, which are gathered again using Eq. (10) to give the wave amplitudes in the real space $A_\alpha(x,t)$. In the pseudo-spectral Fourier expansion (10) we have used a finite number of modes, thus there is a same number of discretized points in the real space. Let us choose a number of these points x_i, consider the wave amplitudes at such points $|A_\alpha(x_i,t)|$. In the dynamical system language, each spatial point can be regarded as a nonlinear oscillator evolving in time according to the partial differential equations (7)–(9). Moreover, due to the diffusive term in (7), these

oscillators are locally coupled, in the sense that each oscillator interacts with its nearest-neighbors.

Previous works have shown the existence of a spatially homogeneous state in this system, undergoing a temporally chaotic evolution. In such a spatially homogeneous state, each spatial point can be regarded as a nonlinear oscillator exhibiting complete synchronization of chaos, i.e.

$$A_\alpha(x_1,t) = A_\alpha(x_2,t) = \cdots = A_\alpha(x_N,t), \quad (16)$$

for all times (the time dependence will be implicitly understood from now on). The existence of this synchronized state can be placed into evidence by drawing return plots of $|A_\alpha(x_i)|$ versus $|A_\alpha(x_j)|$, where x_i and x_j are two distinct points. Considering a fixed x_i for $i = 1$ we have depicted in Figs. 1(a)–1(d), a sample of return plots for sites $j = 8, 16, 24$ and 32, respectively. The control parameter takes on a value $\nu_{2,3} = -1.8$ for which the existence of a spatially homogeneous state has been previously observed. In these return plots, the completely synchronized state is represented by the concentration of points along the main diagonal line $|A_1(x_i)| = |A_1(x_j)|$.
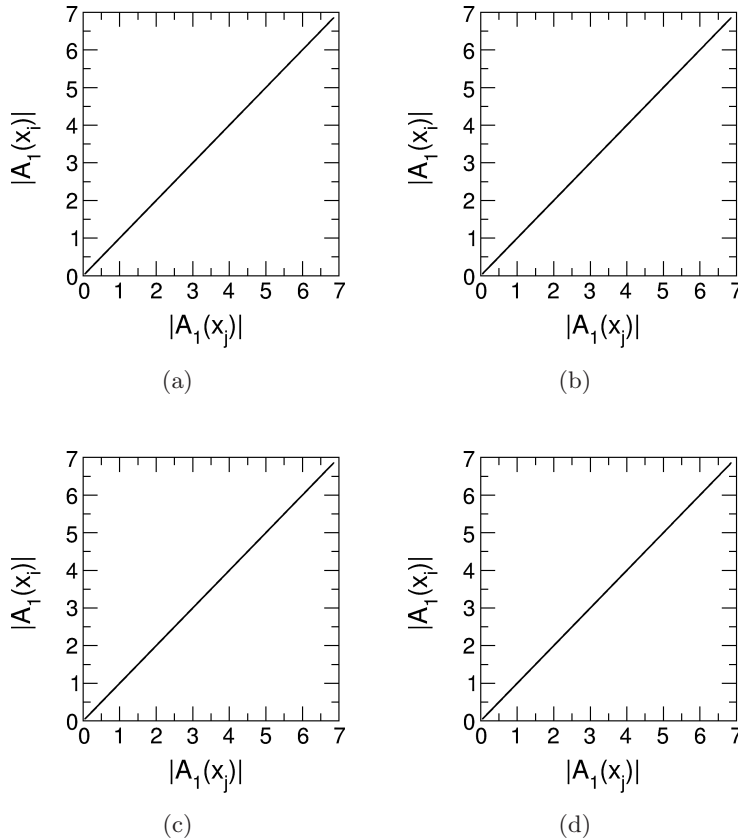

Fig. 1. Return plots of $|A_1(x_i)|$ versus $|A_1(x_j)|$ in the case where the control parameter is $\nu_{2,3} = -1.8$ for $i = 1$ and (a) $j = 8$; (b) $j = 16$; (c) $j = 24$; (d) $j = 32$.
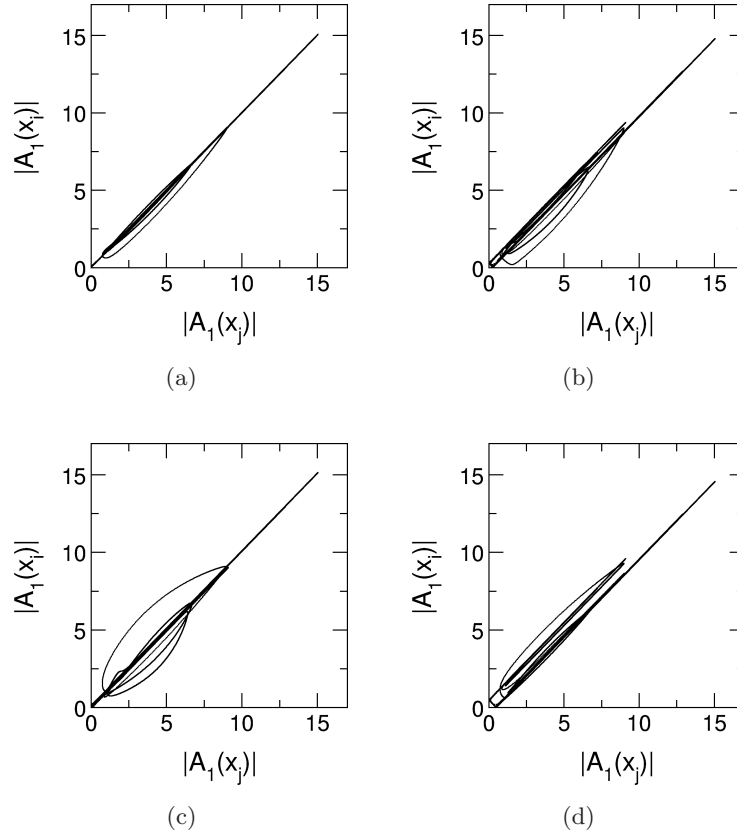
Fig. 2. Return plots of $|A_1(x_i)|$ versus $|A_1(x_j)|$ in the case where the control parameter is $\nu_{2,3} = -3.6$ for $i = 1$ and (a) $j = 8$; (b) $j = 16$; (c) $j = 24$; (d) $j = 32$.

On the other hand, for another value $\nu_{2,3} = -3.6$, we have observed the excitation of spatial modes. Since the dynamics is already chaotic in the homogeneous state, these spatial modes represent a weakly turbulent state, in which we have spatio-temporal chaos. From the point of view of the coupled oscillators, they are no longer synchronized, as illustrated by the return plots of Fig. 2. The excursions of the return plot points out of the diagonal line are thus a manifestation of the spatial mode excitation in the spatially extended system.

Since $A_\alpha(x_j)$ are complex numbers, such that besides the amplitude they can also be described by a phase angle

$$\varphi_{\alpha,n}(t) = \arctan\left\{\frac{\text{Im}[A_{\alpha,n}(t)]}{\text{Re}[A_{\alpha,n}(t)]}\right\}. \quad (17)$$

We remark that this kind of geometric definition of phase is possible here since we have a funnel attractor [Lopes & Chian, 1996] similar to that observed in projections of chaotic trajectories of the Rössler oscillator [Osipov et al., 2003].

A completely synchronized state (16) can be either described by the synchronization of

amplitudes or as the synchronization of the respective phases. In the latter sense, a sensitive diagnostic of synchronization is the complex order parameter introduced by Kuramoto [1984]

$$z_\alpha(t) = R_\alpha(t)\exp(i\Phi_\alpha(t))$$

$$\equiv \frac{1}{N}\sum_{n=-(N/2)+1}^{N/2} \exp(i\varphi_{\alpha,n}(t)), \quad (18)$$

where $R_\alpha(t)$ and $\Phi_\alpha(t)$, $\alpha = 1, 2, 3$, are the amplitude and angle, respectively, of a centroid phase vector for a one-dimensional chain with periodic boundary conditions. Since our attractor is funnel-like the phase is uniquely determined by Eq. (17) and so the Kuramoto order parameter can be accurately determined.

The average of the order parameter magnitude

$$\overline{R_\alpha} = \lim_{T\to\infty} \frac{1}{T}\int_{n=0}^{T} R_\alpha(t)dt, \quad (19)$$

is computed over a time interval large enough to warrant that an asymptotic state has been achieved by the system. A synchronized chaotic state for

all oscillators, signaling a purely temporal dynamics for the spatially homogeneous state, is characterized by $\overline{R_\alpha} = 1$, since there occurs a coherent superposition of the phase vectors with the same amplitude at each time for all discrete spatial locations. The lower is the value of $\overline{R_\alpha}$, the less the spatial coherence of the system state. If the oscillators were completely incoherent, then the phase vectors would be randomly distributed with respect to their angles, such that $\overline{R_\alpha} = 0$ in the limit of infinitely many oscillators. In other words, the breakdown of the totally synchronized state is a criterion for the appearance of spatial modes, which marks the onset of wave turbulence through this bubbling transition.

In Figs. 3(a) and 3(b), we plot the bifurcation diagram for $|A_1(x_1, t)|$ and the average order parameter for the parent wave $\overline{R_1}$, respectively, as a function of the decay rate of the daughter waves $\nu_{2,3}$. Within the numerical accuracy the oscillators lose chaotic synchronization (i.e. there is spatial mode excitation) for values of the decay rate higher than $\nu_{CR} \approx -1.96$, which is the value for which $\overline{R_1}$ ceases to be equal to the unity [Fig. 3(b)]. The (purely temporal) dynamics in the homogeneous manifold can be either periodic or chaotic, as shown by Fig. 3(a): it starts as a period-1 orbit for small

30

(a)

$|A_1(1,t)|$

20

10

0

(b)

$\overline{R_1}$

1

0.95

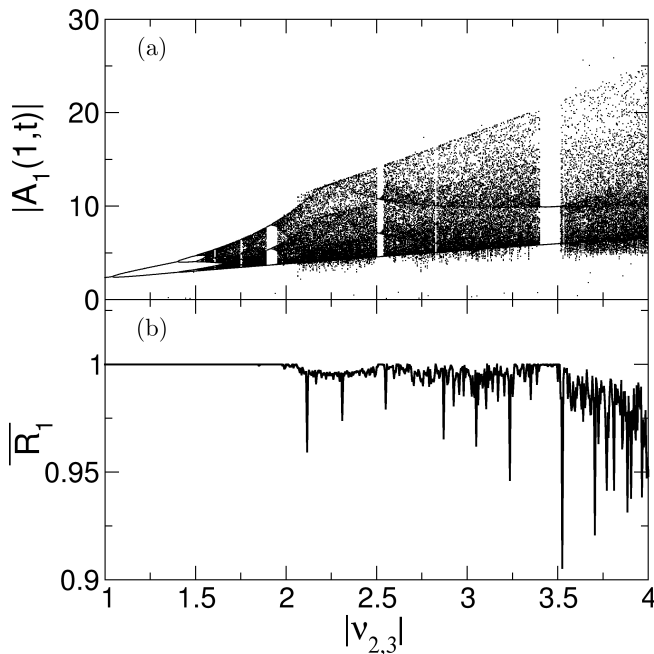0.9

1   1.5   2   2.5   3   3.5   4

$|\nu_{2,3}|$

Fig. 3.   (a) Bifurcation diagram for $|A_1(1,t)|$ as a function of the decay rate $\nu_{2,3}$. (b) Time-averaged order parameter for parent wave versus decay rate for $T = 2 \times 10^5$, after 10^4 transient iterations.
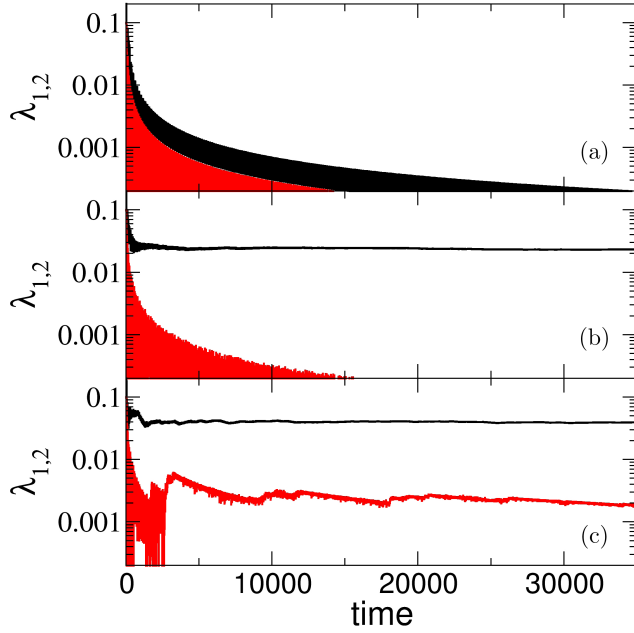
values of $|\nu_{2,3}|$ and undergoes a period-doubling bifurcation cascade to chaotic bands which disappear due to an interior crisis and are followed by a period-3 window. The loss of chaotic synchronization occurs just after a three-band chaotic attractor suffers an internal crisis and merges into a single large chaotic orbit at ν_{CR}.

The dynamics for $\nu_{2,3} < \nu_{CR}$ is mainly chaotic, interspersed with small periodic windows. Most of the chaotic dynamics is associated with the excitation of spatial modes, since the order parameter magnitude there is different from the unity. It is worth emphasizing, though, that chaotic behavior of the oscillators in the spatially homogeneous state is a necessary condition for spatial modes to be excited, since we get $\overline{R_1} = 1$ whenever the dynamics goes periodic. The spatially homogeneous state would act as a kind of stochastic pump, imparting energy to a growing number of spatial modes after the onset of wave turbulence.

A further numerical verification of the loss of synchronization in the spatially homogeneous state is the computation of the Lyapunov spectrum related to the mode dynamics in the Fourier phase space. Since each Fourier mode for the three interacting waves is a degree of freedom in this space, there are $6N$ Lyapunov exponents, computed using Gram–Schmidt reorthonormalization [Wolf *et al.*, 1985; Yamada & Okhitani, 1988]. The largest Lyapunov exponent, denoted as λ_1, refers to the chaotic dynamics in the spatially homogeneous state. If the oscillators are synchronized, they share the same value of λ_1. The second Lyapunov exponent λ_2 is related to the off-synchronized dynamics, or the spatial mode excitation. Since the Lyapunov spectrum is ordered, it suffices that $\lambda_2 > 0$ for the characterization of a spatial mode excitation.

The time evolution of the two largest exponents (out of $6N$ modes considered) is depicted in Fig. 4. When the control parameter $\nu_{2,3}$ takes on values for which the dynamics in the spatially homogeneous state is nonchaotic [Fig. 4(a)] the largest exponent (λ_1) decays to zero as a power-law, which is an indication that asymptotes to zero as the time increases. On the other hand, the second largest exponent (λ_2) decays exponentially to zero, which indicates that it is asymptotically negative. In Fig. 4(b) λ_1 is asymptotically positive, while λ_2 decays to zero as a power-law, hence asymptotes to zero. Hence the dynamics on $\mathcal{M}$ is chaotic and transversely stable. After the excitation of spatial modes [Fig. 4(c)]

Fig. 4. Time evolution of the two largest Lyapunov exponents (λ_1: black points; λ_2: red points) of the dynamical system formed by $6N$ Fourier modes for (a) $\nu_{2,3} = -1.5$; (b) -1.8; (c) -3.6.

the two largest exponents are positive. The ripples observed in the latter figure for λ_2 are due to the long time the trajectory stays in the vicinity of the spatially homogeneous state. Nevertheless, the asymptotic value of λ_2 is positive, meaning that the homogeneous state is transversely unstable.

Moreover, useful information can be obtained from a detailed examination of the second largest exponent, which turns out to be the maximal transversal exponent (λ_2). The fluctuations of the maximal transversal exponent are quantified by the finite time exponent $\tilde{\lambda}_2(t)$, which are computed like those in Fig. 4, but using a finite value of t. The infinite-time limit of $\tilde{\lambda}_2(t)$ equals λ_2. Since the values taken by $\tilde{\lambda}_2(t)$ typically depend on the initial condition, we consider a random sample of initial conditions outside the spatially homogeneous state and compute the corresponding values of $\tilde{\lambda}_2(t)$. Using the recurrent dynamics it suffices to follow a single trajectory of a large number of steps, and the time-t exponents are evaluated from consecutive and nonoverlapping length-t sections of the trajectory [Szezech *et al.*, 2011].

Given such a sequence of values of $\tilde{\lambda}_2(t)$ for, e.g. $t = 300$, we compute the probability distribution function $P(\tilde{\lambda}_2(300))$. In Fig. 5 we show numerical approximations of this probability distribution function for different values of the control parameter
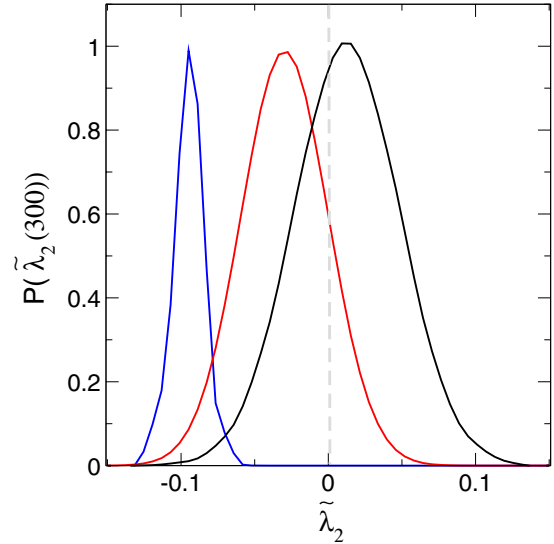

Fig. 5. Probability distribution function of the time-300 maximal transversal Lyapunov exponent for different values of the decay rate of the daughter waves: $\nu_{2,3} = -1.5$ (blue); 1.8 (red); 3.6 (black).

$\nu_{2,3}$. For $\nu_{2,3} = -1.5$ (blue curve in Fig. 5) all the values of $\tilde{\lambda}_2(t)$ are negative, which indicates that the fluctuations of the corresponding exponent represent shrinking distances in phase space with respect to the spatially homogeneous state. As $\nu_{2,3}$ increases, there are also positive fluctuations of these exponents, since there is a positive tail in the corresponding distribution function (red curve in Fig. 5). Such positive fluctuations represent expanding distances with respect to the homogeneous state.

Actually for $\nu_{2,3} \lesssim -1.96$ half of the time-t exponents are positive, which characterizes a blowout bifurcation, i.e. the loss of transversal stability of the spatially homogeneous state. Since the average of the finite-time exponents, for t large enough, is equal to the infinite-time exponent, the blowout bifurcation occurs when the infinite-time (second largest) Lyapunov exponent crosses zero, as the control parameter is varied. If we further increase the latter, the probability distribution drifts slowly towards positive values of $\tilde{\lambda}_2(t)$ (black curve in Fig. 5).

4. Conclusions

The transition to weak wave turbulence in a spatially extended three-wave nonlinearly interacting model has been proved to occur due to the loss of transversal stability of a spatially homogeneous

state undergoing temporally chaotic dynamics. The latter fuels the spatial mode excitation, whose onset is marked by the loss of transversal stability of some periodic orbit embedded in the chaotic attractor representing the spatially homogeneous state. In this work, we analyzed this situation from the point of view of the loss of synchronization of individual oscillators which comprise the spatially homogeneous state. These oscillators come from the discretization of the spatial variable which follows from using a pseudo-spectral method to solve the nonlinear partial differential equations governing the spatiotemporal behavior of the system. The onset of wave turbulence is the point where the oscillators lose phase synchronization, where a geometrical phase has been defined for the motion along the chaotic attractor representing the spatially homogeneous state. We have used, for characterizing this process, a complex order parameter which is extremely sensitive and thus can yield precise estimates of the threshold of weak turbulence in such systems.

We have made a Lyapunov analysis of this system in the Fourier phase space, where each direction refers to a given mode in a spectral decomposition of the wave fields. The spatially homogeneous state represents a three-dimensional subspace in this space, with a chaotic trajectory. The remaining directions are called transversal with respect to this subspace. On ordering the Lyapunov exponents, the maximal one λ_1 refers to an expanding direction in the homogeneous subspace. Since the latter does not allow for a hyperchaotic attractor, however, the second positive one λ_2 is the maximal transversal exponent. We studied the finite-time fluctuations of this transversal exponent and found that the homogeneous subspace loses transversal stability when λ_2 (which is the average of the finite-time fluctuations) crosses zero, which is called a blowout bifurcation.

Acknowledgments

References

Afraimovich, V. S., Verichev, N. N. & Rabinovich, M. I. [1986] "Stochastic synchronization of oscillation in dissipative systems," *Radiophys. Quant. Electron.* **29**, 795–802.

Chian, A. C.-L., Lopes, S. R. & Alves, M. V. [1994] "Generation of auroral whistler-mode radiation via nonlinear coupling of Langmuir waves and Alfven waves," *Astron. Astrophys.* **290**, L13–L16.

Chian, A. C.-L. & Rizzato, F. B. [1994] "Coupling of electromagnetic filamentation instability and electrostatic Langmuir parametric instabilities in laser–plasma interactions," *J. Plas. Phys.* **51**, 61–73.

Chow, C. C., Bers, A. & Ram, A. K. [1992] "Spatiotemporal chaos in the nonlinear three-wave interaction," *Phys. Rev. Lett.* **68**, 3379–3382.

Dyachenko, S., Newell, A. C., Pushkarev, A. N. & Zakharov, V. E. [1992] "Optical turbulence: Weak turbulence, condensates and collapsing filaments in the nonlinear Schrödinger equation," *Physica D* **57**, 96–160.

Frisch, U. [1995] *Turbulence*: *The Legacy of A. N. Kolmogorov* (Cambridge University Press, Cambridge).

Fujisaka, H. & Yamada, T. [1983] "Stability theory of synchronized motion in coupled-oscillator systems," *Prog. Theor. Phys.* **69**, 32–47.

Hindmarch, A. C. [1983] "ODEPACK: A systematized collection of ODE solvers," in *Scientific Computing*, eds. Stepleman, R. S. *et al.* (North-Holland, Amsterdam).

Kaup, D. J., Reiman, A. & Bers, A. [1979] "Space-time evolution of nonlinear three-wave interactions. I. Interaction in a homogeneous medium," *Rev. Mod. Phys.* **51**, 275–309.

Kolmakov, G. V. & Pokrovsky, V. L. [1995] "Stability of weak turbulence spectra in super fluid helium," *Physica D* **86**, 465–469.

Kuramoto, Y. [1984] *Chemical Oscillations, Waves, and Turbulence* (Springer-Verlag, Berlin).

Landau, L. D. & Lifshitz, E. M. [1987] *Fluid Mechanics*, 2nd edition (Pergamon Press, NY).

Lopes, S. R. & Chian, A. C.-L. [1996] "Controlling chaos in nonlinear three-wave coupling," *Phys. Rev. E* **54**, 170–174.

Lopes, S. R. & Rizzato, F. B. [1999] "Nonintegrable dynamics of the triplet–triplet spatiotemporal interaction," *Phys. Rev. E* **60**, 5375–5384.

Li, Y. C. [2007] "Chaos in wave interactions," *Int. J. Bifurcation and Chaos* **17**, 85–98.

Musher, S. L., Rubenchik, A. M. & Zakharov, V. E. [1995] "Weak Langmuir turbulence," *Phys. Rep.* **252**, 177–274.

Newhouse, S., Ruelle, D. & Takens, F. [1978] "Occurrence of strange Axiom-A attractors near quasi periodic flows on T^m, $m \geq 3$," *Comm. Math. Phys.* **64**, 35–40.

Osipov, G. V., Hu, B., Zhou, C., Ivanchenko, M. V. & Kurths, J. [2003] "Three types of transitions to phase synchronization in coupled chaotic oscillators," *Phys. Rev. Lett.* **91**, 024101.

Pecora, L. M. & Carroll, T. L. [1990] "Synchronization in chaotic systems," *Phys. Rev. Lett.* **64**, 821–824.

Picozzi, A. & Haeltermann, M. [2001] "Parametric three-wave soliton generated from incoherent light," *Phys. Rev. Lett.* **86**, 2010–2013.

Pikovsky, A. S., Rosenblum, M. G. & Kurths, J. [2001] *Synchronization*: *A Universal Concept in Nonlinear Sciences* (Springer-Verlag, NY-Berlin-Heidelberg).

Ruelle, D. & Takens, F. [1971] "On the nature of turbulence," *Commun. Math. Phys.* **20**, 167–192.

Rundquist, A., Durfee III, C. G., Chang, Z., Herne, C., Backus, S., Murnane, M. M. & Kapteyn, H. C. [1998] "Phase-matched generation of coherent soft X-rays," *Science* **280**, 1412–1415.

Schröder, E., Andersen, J. S., Levinsen, M. T., Alstrom, P. & Goldburg, W. I. [1996] "Relative particle motion in capillary waves," *Phys. Rev. Lett.* **76**, 4717–4720.

Sridhar, S. & Goldreich, P. [1994] "Towards a theory of interstellar turbulence I: Weak Alfvén turbulence," *Astrophys. J.* **432**, 612–621.

Stegeman, G. I. & Segev, M. [1999] "Optical spatial solitons and their interactions: Universality and diversity," *Science* **286**, 1518–1523.

Szezech Jr., J. D., Lopes, S. R. & Viana, R. L. [2007] "The onset of spatio-temporal chaos in a nonlinear system," *Phys. Rev. E* **75**, 067202-1–4.

Szezech Jr., J. D., Lopes, S. R., Viana, R. L. & Caldas, I. L. [2009] "Bubbling transition to spatial mode excitation in an extended dynamical system," *Physica D* **238**, 516–525.

Szezech Jr., J. D., Lopes, S. R., Caldas, I. L. & Viana, R. L. [2011] "Blowout bifurcation and spatial mode excitation in the bubbling transition to turbulence," *Physica A* **390**, 365–373.

Turner, L. [1996] "Driven-dissipative Eulers equations for a rigid body: A chaotic system relevant to fluid dynamics," *Phys. Rev. E* **54**, 5822–5825.

Wolf, A., Swift, J. B., Swinney, H. L. & Vastano, J. A. [1985] "Determining Lyapunov exponents from a time series," *Physica D* **16**, 285–317.

Yamada, M. & Ohkitani, K. [1988] "Lyapunov spectrum of a model of two-dimensional turbulence," *Phys. Rev. Lett.* **60**, 983–986.

Zakharov, V. E. & Sagdeev, R. Z. [1970] "Spectrum of acoustic turbulence," *Sov. Phys. Dokl.* **15**, 439–441; Russian original: *Dokl. Akad. Nauk. SSSR* **192**, 297–300.

Zakharov, V. E., Dias, F. & Pushkarev, A. [2004] "One-dimensional wave turbulence," *Phys. Rep.* **398**, 1–65.